Journal of Food Protection, Vol. 78, No. 12, 2015, Pages 2108–2116
doi:10.4315/0362-028X.JFP-15-290

Physics of Fresh Produce Safety: Role of Diffusion and Tissue Reaction in Sanitization of Leafy Green Vegetables with Liquid and Gaseous Ozone-Based Sanitizers

MYKOLA V. SHYNKARYK,[1] TARAS PYATKOVSKYY,[1] HUSSEIN M. MOHAMED,[1] AHMED E. YOUSEF,[2] AND SUDHIR K. SASTRY[1]*

[1]*Department of Food, Agricultural, and Biological Engineering, Ohio State University, 590 Woody Hayes Drive, Columbus, Ohio 43210; and* [2]*Department of Food Science and Technology, Ohio State University, 2015 Fyffe Court, Columbus, Ohio 43210, USA*

MS 15-290: Received 8 July 2015/Accepted 14 August 2015

ABSTRACT

Produce safety has received much recent attention, with the emphasis being largely on discovery of how microbes invade produce. However, the sanitization operation deserves more attention than it has received. The ability of a sanitizer to reach the site of pathogens is a fundamental prerequisite for efficacy. This work addresses the transport processes of ozone (gaseous and liquid) sanitizer for decontamination of leafy greens. The liquid sanitizer was ineffective against *Escherichia coli* K-12 in situations where air bubbles may be trapped within cavities. A model was developed for diffusion of sanitizer into the interior of produce. The reaction rate of ozone with the surface of a lettuce leaf was determined experimentally and was used in a numerical simulation to evaluate ozone concentrations within the produce and to determine the time required to reach different locations. For aqueous ozone, the penetration depth was limited to several millimeters by ozone self-decomposition due to the significant time required for diffusion. In contrast, gaseous sanitizer was able to reach a depth of 100 mm in several minutes without depletion in the absence of reaction with surfaces. However, when the ozone gas reacted with the produce surface, gas concentration was significantly affected. Simulation data were validated experimentally by measuring ozone concentrations at the bottom of a cylinder made of lettuce leaf. The microbiological test confirmed the relationship between ozone transport, its self-decomposition, reaction with surrounding materials, and the degree of inactivation of *E. coli* K-12. Our study shows that decontamination of fresh produce, through direct contact with the sanitizer, is more feasible with gaseous than with aqueous sanitizers. Therefore, sanitization during a high-speed washing process is effective only for decontaminating the wash water.

In response to continuing incidents of contamination of fresh produce, the main mitigation strategies for produce such as leafy greens have involved surface decontamination and avoidance of cross-contamination *(8, 21)*. This type of thinking has strongly driven efforts to develop an effective sanitizing agent. A number of liquid sanitizers based on organic acids *(15, 24)*, chlorine *(19)*, biocides *(10, 19)*, ozone *(6, 9, 19, 22)*, and their combinations *(25)* have been proposed. A recently introduced *(17)* liquid sanitizer, FreshRinse, has not mitigated recalls *(5, 12)*.

An often ignored point in the fresh produce and research communities is the physics of produce safety, in particular the rate of penetration of sanitizers to pathogen locations within stomata, crevices, or openings. To be effective, the sanitizer must be able to reach the most inaccessible sites of the target pathogen within the duration of the treatment. Although the lethal effect of liquid sanitizers has been extensively evaluated, it is unclear whether these sanitizers can be successfully delivered to the microorganisms internalized within the product. Bacteria can congregate in a variety of locations in fresh produce, including stomata, cracks in the cuticle, crevices, and pores *(1, 2)*. This variety of niches introduces special challenges, because of the relative inaccessibility of such sites and requires the disinfectant to have great mobility and penetration capability. At present, manufacturers of fresh produce use mostly aqueous sanitizer solutions applied during the washing step *(8, 18)*. To reduce the surface tension and improve sanitizer penetration in stomata and crevices, a wetting agent (surfactant) is frequently added to the washing formulation *(18, 24)*.

Although liquid sanitizers possess certain advantages, most notably their ability to dislodge visible dirt from produce surfaces, their efficacy for reaching deeply internalized microorganisms is questionable. The washing process (particularly with surfactants) opens the possibility that bubbles may become lodged underneath produce in washing flumes, and such bubbles may serve as barriers to contact between sanitizers and internalized microorganisms, rendering treatment ineffective. Thus, despite their touted advantages, surfactant-laden liquid sanitizers cannot compete with the penetration capability of gaseous sanitizers, which have mass diffusivities about four orders of

* Author for correspondence. Tel: 614-292-3508; Fax: 614-292-9448; E-mail: sastry.2@osu.edu.

magnitude greater than those of liquids *(22)* and are (eventually) able to reach most inaccessible sites within produce. Several sanitizers in the gaseous state have been evaluated in recent years, including ozone *(9),* chlorine dioxide *(11),* and cold plasma *(16)*. Of these, ozone was reported to be the most potent, with an oxidation potential of –2.07 V *(22)*.

Despite their greater penetration capability, gaseous sanitizers such as ozone are highly mobile and reactive, which might result in rapid sanitizer depletion due to self-decomposition and reactions with organic and nonorganic matter. A particular concern with sensitive produce such as spinach and lettuce is the possibility of tissue bleaching when sanitizers are not carefully applied; this bleaching could render products sanitary but unsaleable. Thus, the gaseous sanitization process should be considering and analyzed in detail, particularly with regard to the required time for achieving effective treatment and whether and how much sanitizer depletion occurs due to reactions with produce surfaces.

Our goals in this study were (i) to evaluate the time required for efficient sanitization with liquid and gaseous sanitizers, particularly in situations where bubbles may be trapped within cavities; (ii) to develop a mathematical model to predict sanitizer concentration at various produce locations, with and without considering the effect of reaction with produce surfaces; (iii) to experimentally verify the models by comparing predicted and measured ozone concentrations and inactivation of *Escherichia coli* K-12; and (iv) to conduct parametric simulations illustrating the feasibility and challenges associated with liquid and gaseous sanitization.

MATERIALS AND METHODS

Produce. Romaine and green leaf lettuce varieties were used in experiments. Lettuce of good quality was purchased from a local grocery store (Kroger, Columbus, OH) and stored refrigerated at 4°C until used.

Ozone generation, measurement, and decomposition. A corona discharge ozone generator (model LG-14, DEL Ozone, San Luis Obispo, CA) with a maximum flow rate of 10 liters/min and an ozone output of 14 g/h was used in experiments. The generator was supplied with extra dry oxygen at 99.6%. The oxygen inflow rate was controlled with an adjustable 10 liters/min rotameter (Dwyer Instruments, Michigan City, IN) integrated in the generator and monitored with a mass flowmeter (FMA-A2109, Omega Engineering, Atlanta, GA). The ozone/oxygen ratio in the mixture was monitored with either an ozone meter (Mini Hicon, IN USA, Inc., Norwood, MA) or with a spectrophotometer at 253 nm (Spectronic 1201, Milton Roy Co., Rochester, NY). Ozone remaining after treatment was destroyed by a thermal destruct unit (Ozonia, Elmwood Park, NJ).

Efficacy of gas sanitizers and liquid sanitizers under bubble entrapment conditions. To identify potential issues associated with bubble entrapment during washing, capillary tubes were cut to lengths of 0.5 and 1 cm, and each tube was sealed on one end with Cristoseal capillary tube sealant (McCormick Scientific Co., St. Louis, MO). The sealed end was then inoculated with *E. coli* K-12. To simulate bubble entrapment, the tubes were placed in an inverted position in a beaker containing a solution of 200 ppm of chlorine (Clorox, Oakland, CA) and 0.1% sodium dodecyl sulfate (SDS; Sigma-Aldrich, St. Louis, MO). Tubes were allowed to stand in the solution for various periods of time, after which they were removed and survivors enumerated. Gas sanitization of inoculum in similar recessed locations was tested by locating similar tubes in an inverted position within a vessel into which ozone gas (1.5 g/m^3) was introduced at atmospheric pressure and room temperature (~20°C). Samples were withdrawn at various times up to 1 h of treatment time, and survivors were enumerated.

Model for sanitizer transport. Within a crevice or pore in produce, which are typically small, mass transport in a liquid or gas sanitizer can be assumed to be exclusively diffusive. The problem may then be stated as follows:

$$\frac{\partial c}{\partial t} + \nabla \cdot (-D\nabla c) = -R_d \quad (1)$$

where c is the concentration, t is the time, D is the diffusivity, ∇ (Nabla) is the gradient operator, and the term $R_d = k_d c$ is associated with the first-order ozone self-decomposition rate.

The initial condition is that the ozone concentration in the bulk produce, c_o, is 0. At the opening of the channel boundary, a constant ozone concentration c was prescribed. At the liquid-solid interface, two situations were considered. The first was where the reaction with the capillary tube wall was considered negligible, a no-flux boundary condition $\nabla c \cdot \vec{n} = 0$ was specified, where $\vec{n}$ represents the unit normal vector. In the second situation, where the ozone decomposition on the surface of the lettuce leaf was specified as flux through the wall of the lettuce leaf cylinder, the boundary condition was specified as

$$\vec{n}(-D\nabla c) = -R_L \quad (2)$$

The flux was defined as

$$R_L = \gamma F \quad (3)$$

where γ is the probability of ozone uptake and F is the flux of incident molecules. Assuming an ideal gas mixture and low temperature conditions, the collision flux is given by the Hertz-Knudsen equation *(23)*:

$$F = \frac{p_i}{\sqrt{2\pi mkT}} \quad (4)$$

where m is the molecular mass (in kilograms), T is the temperature (K), $p_i = c_i kT$ is the ozone gas partial pressure (Pa), c_i is the ozone gas concentration, and $k = 1.3807 \times 10^{-23}$ (the Boltzmann constant).

A commercial software package, COMSOL 4.2a (Comsol AB, Stockholm, Sweden), was used to simulate the above problem with liquid and gaseous sanitizer. Two types of simulations were conducted. First, a simplified simulation was conducted for model verification using a cylindrical tube geometry, one with inert walls and the other with walls of lettuce leaf (involving wall reaction). Once verified, this model was used for parametric simulations as needed. The second type was a parametric simulation to understand the important variables in crevices and pores of a lettuce head. Romaine and green leaf lettuce heads were cut in half, and the two-dimensional geometry of randomly selected lettuce channels was prepared with Autodesk Inventor software (Autodesk, Inc., San Rafael, CA) and imported into the COMSOL program via the CAD Import Module (Fig. 1). Table 1 provides a summary of simulation conditions and the inputs into the model.

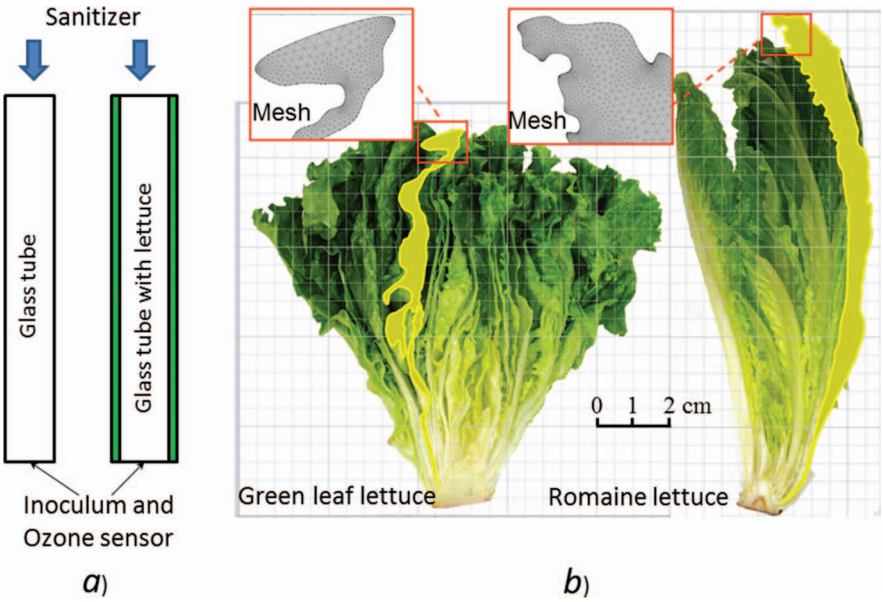

FIGURE 1. *(a) Cylinder geometry used for model verification without cylinder wall reaction (left) and with cylinder wall reaction with the lettuce leaf lining (right). (b) Romaine and green leaf lettuce head cross sections with randomly selected channels used for parametric modeling.*

The unknown quantity is the ozone uptake probability value for the lettuce leaves, which was determined separately by conducting experiments. The partial differential equation (equation 1) subject to the boundary and initial conditions described above was solved in COMSOL using the direct solver. The mesh, consisting of tetrahedral elements, was generated automatically by COMSOL and then manually refined until no significant changes in computed concentration distribution were observed. Analysis was carried out on a computer with an Intel Core i7-980X Extreme processor (Intel Corp., Santa Clara, CA) and 24 GB of RAM working under Windows 7 Ultimate 64bit operating system (Microsoft, Redmond, WA).

Determination of the ozone uptake probability on lettuce leaves. To determine the ozone uptake probability of fresh produce surfaces, a separate experiment was conducted in a specially designed continuous flow reactor integrated into the gaseous ozone treatment setup (Fig. 2). The reactor consisted of a Pyrex glass cylinder (1.12 m long by 0.06 m in diameter; Chemical Scientific Glassblowing Lab, Ohio State University, Columbus) closed with silicone stoppers (size 11.5, Fisher Scientific, Fair Lawn, NJ) on both ends.

The stoppers had openings for inlet and outlet glass tubes. The inlet stopper also had an opening for a tube (closed from one end, 1.3 m long by 0.012 m in diameter) housing a movable rod (1.3 m long by 0.006 m in diameter) coated with lettuce leaves. The reaction time of ozone gas with the lettuce leaf surface was controlled by the length of the exposed rod via a set of external and internal magnets. To eliminate the ozone reaction with unexposed parts of the leaf, an additional flux of oxygen gas (5% of the total flux) was passed through the opening in the rod housing tube.

Mathematical treatment of experimental data was based on the rule of the additivity of kinetic resistances *(3),* according to which the overall decomposition rate on the material surface can be described by the following equation:

$$\frac{1}{k_{obs}} = \frac{1}{k_{kin}} + \frac{1}{k_{dif}} \tag{5}$$

where k_{obs} is the observed rate constant of the ozone decomposition, k_{dif} is the radial diffusion rate constant, and k_{kin} is the reaction limited rate constant. For the reaction under fast flow conditions (Pe >> 1) in a coaxial reactor with an active central rod r_o and passive wall r, the $1/k_{kin}$ and $1/k_{dif}$ values may be expressed by the following equations *(4)*:

$$\frac{1}{k_{dif}} = \frac{r^2}{K_d(q)D_o}p \tag{6}$$

$$\frac{1}{k_{kin}} = \frac{2r}{v_m}\frac{1}{2\gamma/(2-\gamma)}\frac{1-q^2}{q} \tag{7}$$

TABLE 1. *Summary of initial, boundary, and simulation conditions*

Condition	Note	Value	Reference
Initial ozone concn	Bulk concn	$c_o = 0$	
Channel opening boundary	Concn	$c = 0.1$ mol/m^3	
Lettuce leaf walls	Flux	$n\cdot(-D\nabla c) = -R_L$	
	No flux	$n\cdot(-D\nabla c) = 0$	
Diffusivity of ozone in water	At 20°C	$D_W = 1.76 \times 10^{-9}$ m^2/s	*7*
Diffusivity of ozone in oxygen	At 20°C	$D_O = 1.46 \times 10^{-5}$ m^2/s	*13*
Ozone decomposition rate in water	At 20°C	$k_{dw} = 5.78 \times 10^{-4}$ s^{-1}	*9*
Ozone decomposition rate in air	At 20°C	$k_{da} = 2.67 \times 10^{-6}$ s^{-1}	*14*
Ozone molecular mass		$m = 7.97 \times 10^{-23}$ kg	
Ozone uptake probability		Unknown	
Temp		$T = 293.15$ K	

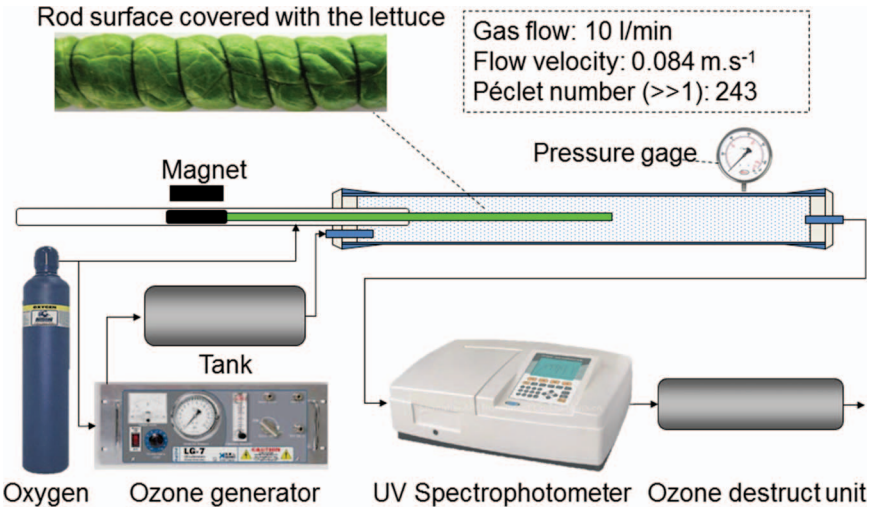

FIGURE 2. *Experimental setup for the ozone uptake probability determination.*

where D_o is the gas-phase diffusivity, K_d is the diffusion rate cell constant for the coaxial reactor, $q = r_o/r$, c is the thermal velocity of ozone molecules, and γ is the probability of ozone uptake. All experimental parameters are summarized in Table 2.

The overall ozone consumption by the produce can be characterized by the uptake probability γ, reflecting a fraction of molecules entrapped (reacted) after collision with its surface. To assess the value of γ, several steps were undertaken: (i) using the coaxial reactor technique, the signal from the spectrophotometer was measured as a function of reaction time (length of the rod coated with lettuce exposed to ozone) and (ii) the first-order reaction rate constant k_{obs} was evaluated by fitting the plot of $\ln(c_o/c)$ versus reaction time t to equation 8:

$$k_{obs} = \frac{\ln(c_o/c)}{t_c} \quad (8)$$

With known k_{obs} and k_{dif}, the value of k_{kin} can be estimated from equation 5, and then the probability of ozone uptake γ is calculated from equation 7.

Model verification. Model verification was conducted by comparison of experimental and simulated ozone concentrations at the bottom of the cylindrical tube (18 mm wide by 90 mm deep, with one end opened as shown in Fig. 1a) with walls made of glass or lettuce leaf, the glass to simulate an inert wall and the leaf to simulate the more realistic case of the produce reacting with the ozone. The cylinder was placed inside a 2-liter stainless steel container with feedthroughs for ozone inlet and outlet lines and fiber-optic cables. The container was supplied with ozone gas for 1 min to reach a target concentration, and then both feedthroughs were closed to minimize convection within the container. Experimental data of ozone concentration were obtained with a spectrophotometer SB4000 (Ocean Optics, Inc., Dunedin, FL) via two open-ended fiber-optic solarization-resistant probes (0.4 mm; Thorlabs, Inc., Newton, NJ) with bare ends aligned 15 mm apart at the bottom of the cylinder. A low pressure mercury lamp (79-7910-1USA, Jelight Company, Inc., Irvine, CA) was used as a light source for measurements. The spectrophotometer was calibrated at 253 nm with the Mini Hicon ozone meter installed at the outlet line of the container. The experimental data were recorded starting when the ozone concentration reached 90% of its maximum value.

TABLE 2. *Experimental parameters for the ozone uptake probability determination*

Parameter	Value	Reference
Radius of central rod covered with lettuce	$r_o = 0.008$ m	
Reactor's passive wall radius	$r = 0.06$ m	
Diffusion rate cell constant for coaxial reactor	$K_d \approx 1.75$	*4*
Diffusivity of ozone in oxygen at 20°C	1.46×10^{-5} m^2/s	*13*
Thermal velocity of ozone molecules	$v_m \approx 360$ m/s	
Gas flow	$v = 10$ liters/min	
Ozone concn	20 g/m^3	

A second set of verification experiments was conducted to determine whether microbiological inactivation was in qualitative agreement with the model. We investigated the ozone transport, self-decomposition, and reaction with produce and the impact of ozone on the *E. coli* K-12 cell suspension. In preparation for experiments, a loop of frozen (–80°C) *E. coli* culture was inoculated into 50 ml of Luria-Bertani (LB) broth (Difco, BD, Sparks, MD) and incubated overnight at 37°C. The next day, culture was transferred into fresh LB broth for second overnight incubation. The bacterial population was determined by spectrophotometric analysis (Spectronic Genesys 5 spectrophotometer, Thermo Fisher Scientific, Waltham, MA) as $\sim 10^9$ CFU/ml. For the experimental evaluation of ozone depletion on produce surfaces and its impact on *E. coli* K-12 inactivation, glass tubes (14 and 16 mm internal diameter by 150 mm long; Kimble Chase, Vineland, NJ) were used. To simulate the ozone reaction with produce, cylinders made of lettuce leaf were introduced inside the tubes of internal diameter 16 mm, reducing the opening to 14 mm; thus, both experiments with and without wall reactions were with tubes of the same dimensions. Before the experiment, small discs (13 mm in diameter, ~0.033 g) were cut out from the lettuce leaf and inoculated with three droplets of *E. coli* K-12 cell suspension (1 μl each). The inoculum was dried for 1 h in a desiccator, and the samples were then placed on the bottom of glass tubes and another two inoculated discs were directly exposed to ozone in a 2-liter stainless steel vessel. The ozone gas was continuously supplied at a concentration of 1.5 g/m^3 for 30 min at 6 liters/min. For the control treatment, inoculated leaves were kept under room conditions. Immediately after treatment, samples were manually stomached in 0.27 ml of peptone water, and decimal dilutions were prepared and plated on sorbitol MacConkey agar plates (Difco, BD). Inoculated plates were incubated for 24 h at 37°C, and the colonies were

enumerated. Average log-transformed microbial reductions were used in the statistical analyses. Comparisons between several groups were conducted using a one-way analysis of variance with Statistica 8.0 (StatSoft, Inc., Tulsa, OK). Tukey's post hoc analysis was then used to analyze mean differences. Differences were considered significant at $P < 0.05$.

RESULTS AND DISCUSSION

Efficacy of gas sanitizers and liquid sanitizers under bubble entrapment conditions. Figure 3 shows a comparison of the inactivation of the *E. coli* K-12 with gaseous ozone (O_3; 1.5 g/m^3) and liquid sanitizer (200 ppm of chlorine with 0.1% SDS) with entrapped bubbles. The suspension was inoculated into different depths (solid symbols, 0.5 cm; open symbols, 1 cm) of each capillary tube.

No significant ($P > 0.05$) reduction in the *E. coli* K-12 counts was observed after immersing inoculated capillary tubes upside down in the liquid sanitizer. Even with the added wetting agent (0.1% SDS), the liquid sanitizer was unable to reach the *E. coli* because of an air bubble that blocked the sanitizer from contacting the inoculum (see Fig. 3 inset). This simple example clearly demonstrates how uncertain sanitization with a liquid sanitizer can be when the pathogen is not easily accessible. However, when gaseous ozone was used, inactivation occurred, with a >1-log reduction in the *E. coli* K-12 population. Although this reduction is far from the inactivation needed, this experiment represents an extreme case involving deep internalization and microbial growth.

Probability of ozone uptake by the lettuce surface. The ozone uptake probability by a fresh produce leaf surface was estimated as described earlier by fitting the plot of $\ln(c_o/c)$ versus the reaction time t. A k_{obs} value of 7.68×10^{-4} s^{-1} was obtained for the given experimental condition. The radial diffusion rate constant k_{dif} was 3.96×10^{-2} s^{-1}, indicating a reaction rate–controlled heterogeneous reaction. With known k_{obs} and k_{dif}, a k_{kin} value of 8×10^{-4} s^{-1} was estimated from equation 5. The measured reaction rate of the ozone decomposition on the surface of the lettuce was of the same order of magnitude as the reported ozone self-decomposition rate in tap water *(9)*. The uptake probability $\gamma = 6.57 \times 10^{-7}$ was calculated from equation 7. The estimated value represents an effective reaction probability assuming a smooth surface.

Impact of the uptake probability. Assuming that the uptake probability γ is constant over time, a simulation taking into account the ozone–lettuce surface interaction was undertaken. Figure 4 shows the steady-state ozone concentration in the bottom (far) corner of a rectangular channel for different combinations of channel depth and width. In this figure, both geometric parameters range from 1 to 100 mm.

In the simulation, the ozone concentration at the targeted depth dropped significantly with increasing channel depth and decreasing width. For example, for a channel 5 mm wide, about 80% of the ozone would be consumed before it reached a depth of 50 mm. For a channel 1 mm wide, at the same depth of 50 mm only 2% of the initial sanitizer concentration remained. A significant reduction in ozone concentration occurred even for the widest channel opening of 100 mm. At a depth of 100 mm, about 50% of the ozone would be lost. This result suggests that it may be beneficial to add convective transport when designing treatment chambers for redistributing ozone within produce.

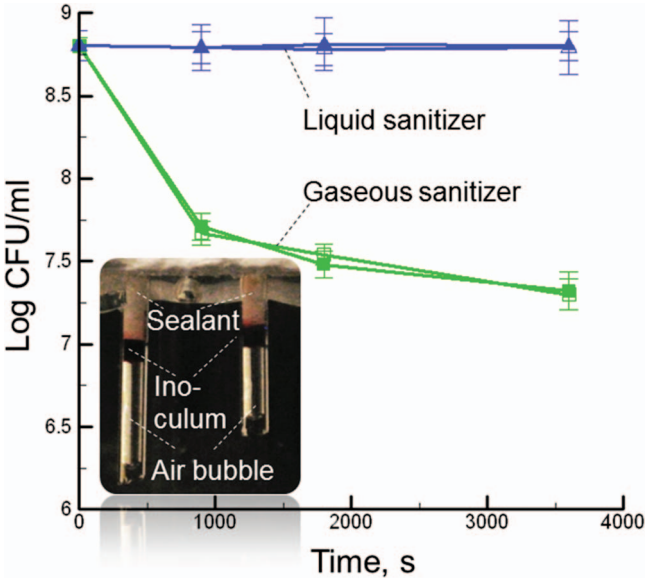

FIGURE 3. *Inactivation rate of* Escherichia coli *K-12 suspension inoculated into capillary tubes at different depths (solid symbols, 0.5 cm; open symbols, 1 cm) and exposed to gaseous sanitizer (ozone at 1.5 g/m^3) and liquid sanitizer (200 ppm of chlorine with 0.1% SDS). Error bars indicate standard deviations.*

Model verification. Figure 5 shows a comparison between simulated and experimentally obtained ozone concentrations during diffusion to the bottom of the glass tube. The simulation was conducted without taking into account any reaction with the tube walls, and the glass tube and vessel were assumed to not react with the ozone. The dashed line corresponds to the ozone concentration inside the container in the presence of the sample. It took about 1 min for the ozone concentration in the container to reach the maximum value. The concentration of the ozone remained practically unchanged (<3% decrease) during the studied time period. An overall good agreement was observed between experimental and simulated data. Both curves reached a plateau after about 1,000 s. The plateau of the experimental curve was slightly below the maximum initial ozone concentration, which could have been because of decomposition of the ozone. The difference in the initial and intermediate stages of diffusion for the experiment and simulation was related to the time required to reach the target concentration of ozone and the presence of some convective and gravitational forces.

Figure 6 shows data obtained for a diffusion experiment with lettuce leaf and simulated data from the model taking into account a reaction with the produce surface. The dashed line corresponds to ozone concentration inside the container in the presence of the sample. As for the glass tube, no

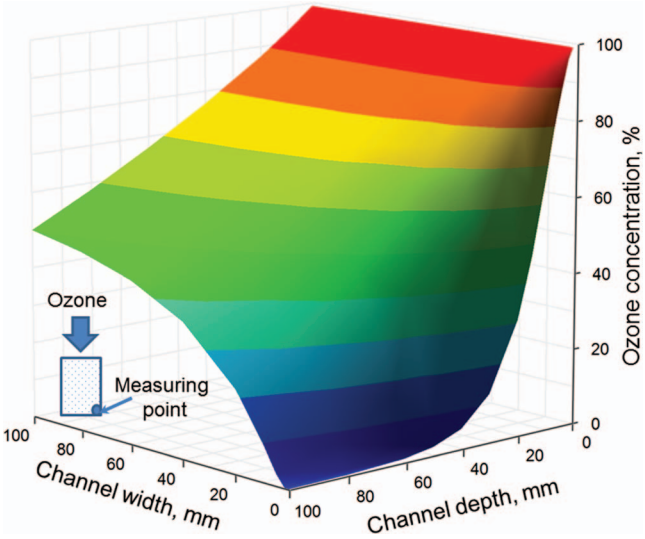

FIGURE 4. *Simulated surface plot of the ozone equilibrium concentration in the bottom corner of a rectangular channel versus channel width and depth, calculated from the model.*

significant change in the ozone concentration inside the vessel was observed. Two separate experiments were conducted, one with fresh leaf (first run) and another with the same leaf previously exposed to ozone for 1 h (second run).

The ozone concentration for the fresh sample increased far more slowly than for the preexposed sample (Fig. 6), and the final ozone concentration after 2,000 s was higher for the second run, which is related to the decreased reaction probability of ozone with the surface of the lettuce after the first treatment. The rate of reaction with the produce is initially at its maximum level and then decreases as the surface tissue reacts with the ozone. Our experiments for measurement of the reaction probability were conducted for relatively brief periods (seconds), whereas the current treatments lasted 0.5 h. Thus, the reaction rate may be

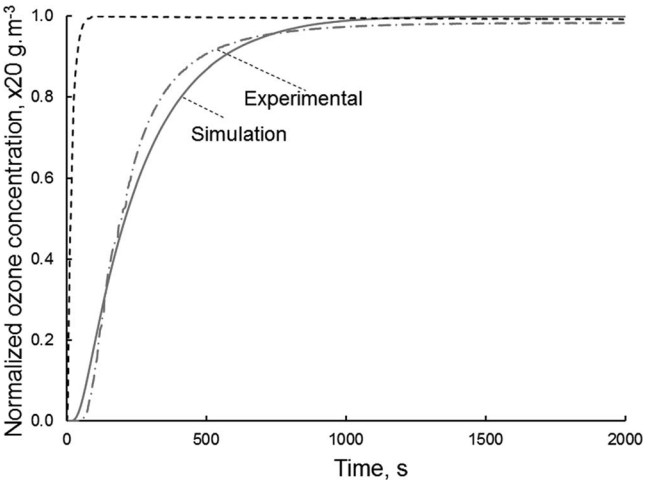

FIGURE 5. *Simulated and experimentally obtained ozone concentration at the bottom of a tube (18 mm wide and 90 mm deep) during ozone diffusion without reaction with tube walls. The dashed line shows ozone concentration inside the vessel.*

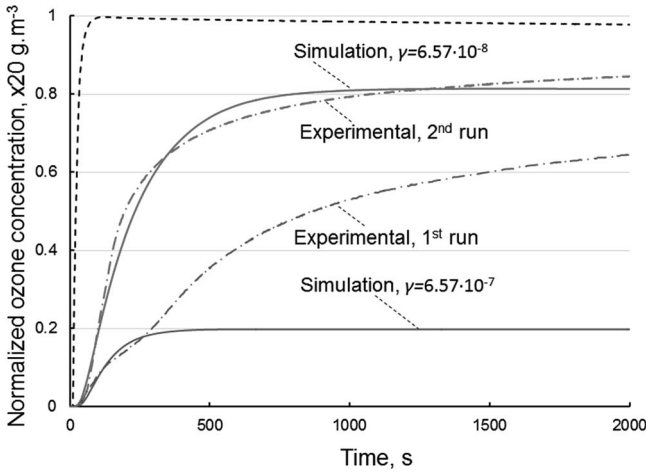

FIGURE 6. *Simulated and experimentally obtained ozone concentration at the bottom of tube (18 mm wide and 90 mm deep) during ozone diffusion with reaction with tube walls (lettuce) taken into account. The dashed line shows ozone concentration inside the vessel.*

expected to decrease over time as the tissue reaction proceeds, resulting in improved ozone delivery to deeply internalized pathogen sites. However, such tissue reaction must not cause undesirable changes in the visual appearance of the produce, rendering it unattractive. The question of produce appearance will be dealt with separately in another study from our group.

The model with the uptake probability $\gamma = 6.57 \times 10^{-7}$ had good agreement with the first run experimental curve during the first 2 to 3 min of the experiment, reaching the plateau at about 20% of the ozone concentration inside the vessel. Such behavior was expected because the model assumed a constant reaction probability measured at the early stages of the reaction. The model with a 10 times lower uptake probability ($\gamma = 6.57 \times 10^{-8}$) had good agreement with the experimental data obtained for the sample previously exposed to ozone for 1 h. Thus, the reaction probability of ozone with lettuce surfaces can drop by one order of magnitude during sanitization when the ozone availability exceeds its demand. In both cases, the plateau was not reached within the studied time period.

Experimental validation of *E. coli* K-12 inactivation by ozone. Figure 7 illustrates the inactivation of *E. coli* K-12 with gaseous ozone on inoculated leaf discs directly exposed to ozone and placed inside glass tubes with or without an internal cylinder made of lettuce leaf.

The initial mean (±standard deviation) *E. coli* K-12 count was 8.1 ± 0.1 log CFU/g for wet inoculum. Drying of the inoculum for 1 h somewhat inhibited the recovery of the inoculated population, yielding 7.6 ± 0.3 log CFU/g. Ozone treatment of directly exposed lettuce samples reduced *E. coli* K-12 colony counts by 1.4 log CFU/g, whereas treatment of samples inside glass tubes produced a reduction of 1.2 log CFU/g. The data analysis, however, revealed no significant differences ($P > 0.05$) between colony counts for these two treatments. For the directly exposed sample surface, the

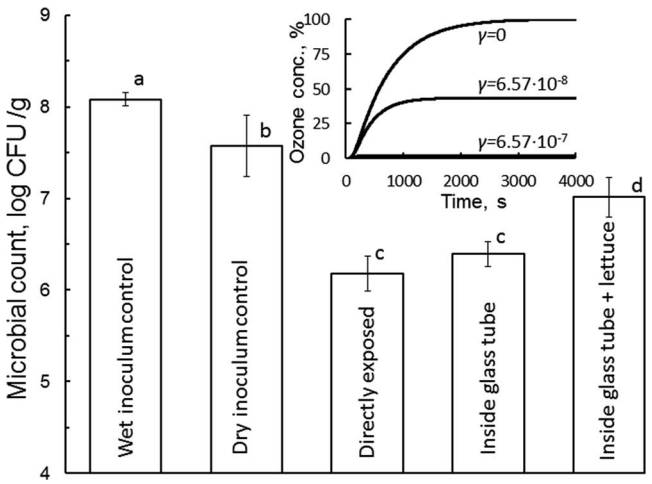

FIGURE 7. E. coli *K-12 inactivation after 30 min of exposure to ozone at 1.5 g/m*^{3}. *Values for bars with different letters are significantly different (*$P < 0.05$). *Error bars indicate standard deviations. Inset: model prediction of ozone concentration at the closed end of the tube (as percentage of original vessel concentration) over time, at different reaction probabilities (*γ).

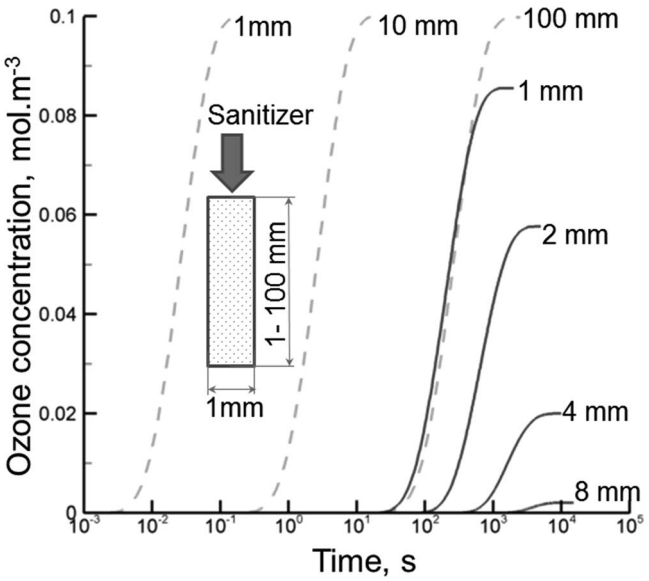

FIGURE 8. *Simulated ozone concentration change at different depths of a rectangular channel (1 mm wide) for aqueous (solid lines) and gaseous (dashed lines) ozone sanitizers.*

come-up time is practically instantaneous, thus the extent of inactivation may be estimated from the data of Figure 3, which shows an approximately 1.3-log reduction in cell population. The ozone treatment in the present study resulted in a 1.4-log reduction, which is in close agreement with predictions. For the samples within glass tubes, the model for ozone concentration at this point (Fig. 3 inset; $\gamma = 0$) shows the predicted come-up time for ozone concentration. The ozone concentration approaches 75% of its steady-state value in just under 1,000 s, and values slowly approach the steady state thereafter. This treatment translated to a 1.2-log reduction, which, although not significantly different from the results for the directly exposed samples, is qualitatively attributable to the lower ozone concentration over the 0.5-h study duration. These results suggest that even after ozone reaches the pathogen location, a sufficient reaction time must be provided to ensure inactivation.

Insertion of a lettuce cylinder into the glass tube with the sample on the bottom significantly affected ($P < 0.05$) the inactivation of *E. coli* K-12, reducing the total inactivation to only 0.6 log CFU/g. This result clearly shows the impact of ozone depletion on *E. coli* inactivation through diffusion and reaction with the produce surface. Again, the model predictions are in qualitative agreement. For the early stages, little or no ozone is delivered to the pathogen site (see Fig. 7 inset, curve for $\gamma = 6.57 \times 10^{-7}$). However, over time as the reaction with tissue proceeds, more and more ozone is delivered to the pathogen site (see Fig. 7 inset, curve for $\gamma = 6.57 \times 10^{-8}$). However, overall the ozone concentration was always lower than that for the inert tubes, thus confirming that the model prediction is in qualitative agreement with experiment.

A detailed quantitative microbiological assessment was not attempted in the present study because lengthy experimentation would be required to determine tissue reaction rates over time and a detailed characterization of *E. coli* K-12 inactivation kinetics under ozone treatment would be needed. Nevertheless, the results obtained in this study reveal that the general inactivation trends may be predicted by diffusion-reaction models.

Impact of sanitizer state and diffusivity. The state of the sanitizer determines its two major characteristics: stability and mobility. For ozone-based sanitizers, the difference in these characteristics between the gaseous ozone and the ozone dissolved in water is highly significant. The diffusivity of ozone molecules in water is about four orders of magnitude lower than that of the gaseous state ($\sim 1.76 \times 10^{-9}$ versus $\sim 1.46 \times 10^{-5}$ m^2/s at 20°C) *(7, 13)*, the half-life of ozone in an aqueous medium is about two orders of magnitude shorter than that of the gaseous state ($\sim 1.2 \times 10^3$ versus $\sim 2.6 \times 10^5$ s at 20°C) *(9, 14)*. In practical terms, these two parameters will affect the time required for sanitizer to reach the microorganism and the final sanitizer concentration when contact occurs. Assuming that sanitizer is delivered to the opening of a rectangular pore 1 mm wide with a depth of 1 to 100 mm and filled with gas and water, the ozone infiltration can be simulated. Figure 8 shows the change in ozone concentration at different depths of a 1-mm-wide rectangular channel for the liquid and gaseous ozone. In this example, the transport was assumed to be by diffusion with no reaction with surfaces, $n \cdot (-D \nabla c) = 0$.

The difference in time required for molecules of ozone to reach the same depth of 1 mm in gaseous and liquid medium is proportional to the difference in diffusivity of the medium (about four orders of magnitude). The gaseous ozone can reach equilibrium at 1 mm depth practically instantly ($\sim 10^{-1}$ s). In contrast, the liquid ozone reaches equilibrium in about 15 min, and when the plateau is reached about 15% of the ozone has been depleted due to the self-decomposition. In the same amount of time (15 min),

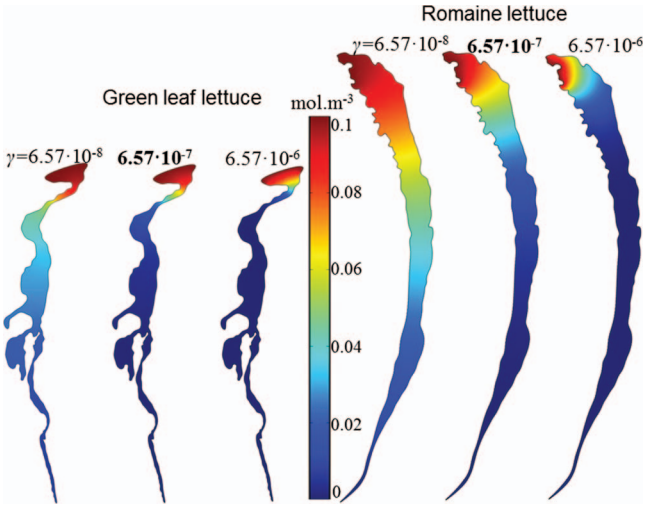

FIGURE 9. *Simulated gaseous ozone penetration into individual channels of romaine and green leaf lettuce at different reaction probabilities.*

the gaseous sanitizer can reach a depth of 100 mm without any depletion. For liquid sanitizer, significant more time is required to reach equilibrium, and a decrease in ozone concentration occurs as the theoretical pathogen internalization depth increases. At 8 mm depth, practically all ozone is decomposed within the penetration time, which exceeds several hours. Hence, when pathogens are internalized deeper than 1 mm in leaf surface macro structures in the presence of a water barrier, the efficacy of short time inactivation with water-based sanitizers might be questionable. This observation with ozone can be expanded to chlorine and other water-based sanitizers because diffusivity of the active components in aqueous solutions is comparable *(20)*. The current industry practice of using short duration washing and decontamination (often <1 min duration) may be insufficient to assure inactivation of internalized bacteria.

Impact of the lettuce head matrix. Figure 9 provides a comparison of the penetration of gaseous ozone into individual channels of romaine and green leaf lettuce heads (see also Fig. 1). A steady-state simulation was conducted for a two-dimensional geometry assuming constant ozone concentration at the opening on the top of the lettuce head. The reaction with the leaf surface was taken into account, and in addition to the measured reaction probability ($\gamma = 6.57 \times 10^{-7}$) simulations were also performed for probabilities that were one order of magnitude higher and lower than the measured value.

Comparing ozone penetration into individual channels at the same reaction probability, romaine lettuce is more accessible and ozone penetrates more deeply. However, a channel contraction next to the opening significantly reduces penetration depth in green leaf lettuce. In both cases, a narrow tail at the bottom of the channel remains practically inaccessible, even for ozone. This gas behavior is consistent with the information shown in Figure 4, as the distance between walls reduces to 1 to 2 mm. The current simulation presents a worst-case scenario when gas can penetrate only from the top of the lettuce head. However, in actual three-dimensional lettuce heads multiple openings occur on the sides and bottom of the head.

Evaluation of the reaction probability reveals its significant impact on the depth of ozone penetration into the lettuce head channels. For a onefold higher than measured probability, the ozone is quickly consumed by the channel walls, and penetration depth is limited to about 10 to 20 mm below the channel opening for both geometries. Reduction of the reaction probability by one order of magnitude significantly improves penetration, enabling the sanitizer to reach the tail area of the channel.

According to simulations and experimental results, when designing a sanitization step for a particular product the processor must consider both the inactivation capability of disinfectant and its characteristics, including stability, reaction kinetics with product, and transport properties. Even the most potent sanitizer is unable to kill a pathogen unless the sanitizer and pathogen can come into contact. Thus, sanitizing time must be long enough to permit sanitizer diffusion into product crevices, which can provide a shelter for bacteria. Mathematical models, once verified, can be useful tools for designing such processes. Sanitization time differs significantly depending on the sanitizer state. For aqueous ozone sanitizer, the time required for diffusion competes with the rate of ozone self-decomposition, limiting the ozone penetration to several millimeters. For gaseous ozone, penetration depth is mainly limited by self-decomposition on product surfaces and decreases with reduction in channel width. Further study is required to assess the impact of different processing conditions (e.g., temperature, humidity, presence of moisture, and dust on leaf surfaces) on ozone-product reaction kinetics. Our studies were designed to represent extreme conditions of deep internalization. In general, internalization may be at much shallower depths; thus, the prospect for gaseous sanitization in such cases is far more optimistic. These results indicate that the use of liquid sanitizers in a high-speed washing situation is not useful for decontamination of fresh produce, except for dislodging visible dirt from produce surfaces and for decontaminating the wash water being recycled during the work shift. For dirt-free produce with modest levels of internalized pathogens, gaseous sanitizer treatment represents a more viable option.

ACKNOWLEDGMENTS

Financial and research support was provided in part by U.S. Department of Agriculture, National Institute of Food and Agriculture grant 2009-51110-05902 and in part by the Ohio Agricultural Research and Development Center, College of Food, Agricultural and Environmental Sciences, Ohio State University. References to commercial products or trade names are made with the understanding that no endorsement or discrimination by Ohio State University is implied.

REFERENCES

1. Erickson, M. C. 2012. Internalization of fresh produce by foodborne pathogens. *Ann. Rev. Food Sci. Technol.* 3:283–310.
2. Erickson, M. C., C. C. Webb, J. C. Diaz-Perez, S. C. Phatak, J. J. Silvoy, L. Davey, A. S. Payton, J. Liao, L. Ma, and M. P. Doyle.

2010. Infrequent internalization of *Escherichia coli* O157:H7 into field-grown leafy greens. *J. Food Prot.* 73:500–506.
3. Frank-Kameneckij, D. A., and N. Thon. 1955. Diffusion and heat exchange in chemical kinetics. Princeton University Press, Princeton, NJ.
4. Gershenzon, Y. M., V. M. Grigorieva, A. V. Ivanov, and R. G. Remorov. 1995. O_3 and OH sensitivity to heterogeneous sinks of HO_x and CH_3O_2 on aerosol particles. *Faraday Discuss.* 100:83–100.
5. Gillespie, C. 2012. Fresh Express spinach recall is the sixth in 16 months. Available at: http://foodpoisoningbulletin.com/2012/fresh-express-spinach-recall-is-the-sixth-in-16-months/. Accessed 30 June 2015.
6. Hunt, N. K., and B. J. Marinas. 1999. Inactivation of *Escherichia coli* with ozone: chemical and inactivation kinetics. *Water Res.* 33:2633–2641.
7. Johnson, P. N., and R. A. Davis. 1996. Diffusivity of ozone in water. *J. Chem. Eng. Data* 41:1485–1487.
8. Jongen, W. (ed.). 2005. Improving the safety of fresh fruit and vegetables. CRC Press, Boca Raton, FL.
9. Khadre, M. A., A. E. Yousef, and J. G. Kim. 2001. Microbiological aspects of ozone applications in food: a review. *J. Food Sci.* 66:1242–1252.
10. Knowles, J., and S. Roller. 2001. Efficacy of chitosan, carvacrol, and a hydrogen peroxide–based biocide against foodborne microorganisms in suspension and adhered to stainless steel. *J. Food Prot.* 64:1542–1548.
11. Lee, S.-Y., M. Costello, and D.-H. Kang. 2004. Efficacy of chlorine dioxide gas as a sanitizer of lettuce leaves. *J. Food Prot.* 67:1371–1376.
12. Limbach, J. 2014. Fresh Express recalls Italian salad. Available at: http://www.consumeraffairs.com/salad-recalls. Accessed 30 June 2015.
13. Massman, W. J. 1998. A review of the molecular diffusivities of H_2O, CO_2, CH_4, CO, O_3, SO_2, NH_3, N_2O, NO, and NO_2 in air, O_2 and N_2 near STP—polar and polyatomic gases. *Atmos. Environ.* 32:1111–1127.
14. Okafor, N. 2011. Environmental microbiology of aquatic and waste systems. Springer, New York.
15. Ortega, Y. R., M. P. Torres, and J. M. Tatum. 2011. Efficacy of levulinic acid sodium dodecyl sulfate against *Encephalitozoon intestinalis, Escherichia coli* O157:H7, and *Cryptosporidium parvum*. *J. Food Prot.* 74:140–144.
16. Perni, S., G. Shama, and M. G. Kong. 2008. Cold atmospheric plasma disinfection of cut fruit surfaces contaminated with migrating microorganisms. *J. Food Prot.* 71:1619–1625.
17. Powell, D. 2011. Fresh Express marketing missteps 2.0. Available at: http://barfblog.com/2011/05/fresh-express-marketing-missteps-2-0. Accessed 30 June 2015.
18. Sapers, G. M. 2003. Washing and sanitizing raw materials for minimally processed fruit and vegetable products, p. 221–246. *In* J. S. Novak, G. M. Sapers, and V. K. Juneja (ed.), Microbial safety of minimally processed foods. CRC Press, Boca Raton, FL.
19. Singh, N., R. K. Singh, A. K. Bhunia, and R. L. Stroshine. 2002. Efficacy of chlorine dioxide, ozone, and thyme essential oil or a sequential washing in killing *Escherichia coli* O157:H7 on lettuce and baby carrots. *LWT Food Sci. Technol.* 35:720–729.
20. Tang, A., and O. C. Sandall. 1985. Diffusion coefficient of chlorine in water at 25–60°C. *J. Chem. Eng. Data* 30:189–191.
21. U.S. Food and Drug Administration. 2001. Analysis and evaluation of preventive control measures for the control and reduction/elimination of microbial hazards on fresh and fresh-cut produce executive summary. Available at: http://www.fda.gov/Food/FoodScienceResearch/SafePracticesforFoodProcesses/ucm091016.htm. Accessed 30 July 2015.
22. Vurma, M., R. B. Pandit, S. K. Sastry, and A. E. Yousef. 2009. Inactivation of *Escherichia coli* O157:H7 and natural microbiota on spinach leaves using gaseous ozone during vacuum cooling and simulated transportation. *J. Food Prot.* 72:1538–1546.
23. Woodruff, D. P., and T. A. Delchar. 1994. Modern techniques of surface science. Cambridge University Press, Cambridge.
24. Zhao, T., P. Zhao, and M. P. Doyle. 2009. Inactivation of *Salmonella* and *Escherichia coli* O157:H7 on lettuce and poultry skin by combinations of levulinic acid and sodium dodecyl sulfate. *J. Food Prot.* 72:928–936.
25. Zhou, F., B. Ji, H. Zhang, H. Jiang, Z. Yang, J. Li, J. Li, Y. Ren, and W. Yan. 2007. Synergistic effect of thymol and carvacrol combined with chelators and organic acids against *Salmonella Typhimurium*. *J. Food Prot.* 70:1704–1709.